PITX2 knockout induces key findings of electrical remodelling as seen in persistent atrial fibrillation

Carl Schulz[1,2,*], MD Marc D. Lemoine[1,2,3,*], PhD Giulia Mearini[1,2,4], PhD Jussi Koivumäki[5], Jascha Sani[1,2], PhD Edzard Schwedhelm[2,6], MD Paulus Kirchhof[2,3,7], PhD Amer Ghalawinji[8], MD Monika Stoll[8,9], MD Arne Hansen[1,3], MD Thomas Eschenhagen[1,3,*], MD Torsten Christ[1,3,*]

[1]Institute of Experimental Pharmacology and Toxicology, University Medical Center Hamburg-Eppendorf, Hamburg, Germany;

[2]DZHK (German Centre for Cardiovascular Research), partner site Hamburg/Kiel/Lübeck, Hamburg, Germany;

[3]Department of Cardiology, University Heart and Vascular Center, Hamburg, Germany;

[4]DiNAQOR AG, Pfäffikon, Switzerland;

[5]BioMediTech, Faculty of Medicine and Health Technology, Tampere University, Tampere, Finland;

[6]Institute of Clinical Pharmacology and Toxicology, University Medical Center Hamburg-Eppendorf, Hamburg, Germany;

[7]Institute of Cardiovascular Sciences, College of Medical and Dental Sciences, University of Birmingham, UK;

[8]Institute of Human Genetics, Division of Genetic Epidemiology, University of Münster, Münster, Germany;

[9]Department of Biochemistry, CARIM School for Cardiovascular Sciences, Maastricht University, Maastricht, The Netherlands;

*Contributed equally

Address for correspondence

PD Dr. med Torsten Christ

Institute of Experimental Pharmacology and Toxicology

University Medical Centre Hamburg-Eppendorf

Martinistraße 52

20246 Hamburg

Telefon: 040-7410-52414

Fax: 040-7410-54876

E-Mail: t.christ@uke.de

or

Carl Schulz

Institute of Experimental Pharmacology and Toxicology

University Medical Centre Hamburg-Eppendorf

Martinistraße 52
20246 Hamburg
Telefon: 040-7410-52414
Fax: 040-7410-54876
E-Mail: carlschulz@freenet.de

Running title

PITX2 knock out in atrial hiPSC-CM

Abstract

Background

Electrical remodelling in human persistent atrial fibrillation (AF) is believed to result from rapid electrical activation of the atria, but underlying genetic causes may contribute. Indeed, common gene variants in an enhancer region close to *PITX2* are strongly associated with AF, but the mechanism behind this association remain unknown. This study evaluated consequences of PITX2 deletion in human induced pluripotent stem cell derived atrial cardiomyocytes (hiPSC-aCM).

Methods

CRISPR/Cas9 was used to delete *PITX2* ($PITX2^{-/-}$) in a healthy human iPSC line which served as isogenic control. HiPSC-aCM were differentiated with unfiltered retinoic acid (RA) and cultured in atrial engineered heart tissue (aEHT). Force and action potential were measured in aEHTs. Single hiPSC-aCM were isolated from aEHT for ion current measurements.

Results

$PITX2^{-/-}$ aEHT beat slightly slower than isogenic control without irregularity. Force was lower in $PITX2^{-/-}$ than in isogenic control (0.053±0.015 vs. 0.131±0.017 mN, n=28/3 vs. n=28/4, $PITX2^{-/-}$ vs. isogenic control; $p<0.0001$), accompanied by lower expression of CACNA1C and lower L-type Ca^{2+} current density. Early repolarisation was weaker (APD_{20}; 45.5±13.2 vs. 8.6±5.3 ms, n=18/3 vs. n=12/4, $PITX2^{-/-}$ vs. isogenic control; $p<0.0001$) and maximum diastolic potential was more negative (-78.3±3.1 vs. -69.7±0.6 mV, n=18/3 vs. n=12/4, $PITX2^{-/-}$ vs. isogenic control; $p=0.001$), despite normal inward rectifier currents (both I_{K1} and $I_{K,ACh}$) and carbachol-induced shortening of APD.

Conclusions

Complete PITX2 deficiency in hiPSC-aCM recapitulates some findings of electrical remodelling of AF in the absence of fast beating, indicating that these abnormalities could be primary consequences of lower PITX2 levels.

Keywords

Atrial fibrillation, remodelling, PITX2, hiPSC-CM, engineered heart tissue, calcium currents

Non-standard Abbreviations and Acronyms

AF	atrial fibrillation
aEHT	atrial engineered heart tissue
AP	action potential
APA	action potential amplitude
APD	action potential duration
CCh	carbachol
CM	cardiomyocyte
dV/dt_{max}	maximum upstroke velocity
EHT	engineered heart tissue
GWAS	genome-wide association study
hiPSC	human-induced pluripotent stem cells
hiPSC-aCM	human induced pluripotent stem cell-derived atrial cardiomyocyte
hiPSC-CM	human induced pluripotent stem cell-derived cardiomyocyte
I_{Ca}	calcium current
I_{Kur}	ultrarapid delayed rectifier potassium current
I_{Kr}	rapid delayed rectifier potassium current
I_{K1}	inward rectifier potassium current
MDP	maximum diastolic potential
PITX2	paired-like homeodomain transcription factor 2
$PITX2^{-/-}$	PITX2 knock out
RA	retinoic acid
RMP	resting membrane potential
SR	sinus rhythm
$V_{Plateau}$	plateau voltage
4-AP	4-aminopyridine

Introduction

Atrial fibrillation (AF) is the most common arrhythmia and affects approximately 1% of the population with increasing incidence and substantial morbidity.[1] Much of the current understanding of the pathophysiology of human AF originates from work with isolated atrial tissues/cells obtained from patients during open heart surgery.[2] AF is frequently associated with structural heart diseases that stretch the atria as typically seen in mitral stenosis[3] but much more common in heart failure when end-diastolic pressure is raised.[4] It therefore remains unclear what may proceed and/or facilitate early onset AF without risk factors.

Genome wide association studies (GWAS) have identified nearly 140 genetic loci associated with AF,[5] located near genes coding for ion channels, developmental transcription factors, structural remodelling and cytoskeletal proteins. Functional effects of such gene variants should help to identify targets involved in AF initiation and/or subsequent remodelling. Gene variants in a gene desert on chromosome 4q25, 175 kilobases upstream of the gene encoding for the transcription factor PITX2 (paired-like homeodomain transcription factor 2) showed the strongest association with AF.[6–8] However, the relation between variants, PITX2 gene transcription and abundance and AF appears to be complex and remains only partially understood. In adequately powered studies, AF-associated variants were not associated with differences in PITX2 abundance in human atrial biopsies.[9,10] On the other hand, a significant number of AF patients showed reduced PITX2 levels in the left atrium with large interindividual differences.[5,6]

Mouse models have been used to study functional aspects of PITX2 gene deletion ("knock-out").[11,12,13,14] While global deletion of PITX2 was lethal,[15] homozygous atrial-specific knock-out mice (NPPA-Cre model) showed dysregulation of several genes involved in excitation-contraction coupling, including downregulation of *CACNA1C*, which was associated with reduced L-type calcium currents.[11] A global heterozygous knock-out mouse showed 40% lower than wildtype PITX2 abundance, shorter action potentials and increased AF-inducibility.[10] The data are compatible with a primary contribution of PITX2 deficiency to AF.

However, substantial differences exist in atrial electrophysiology between mouse and human.[16] Human induced pluripotent stem cell-derived cardiomyocytes (hiPSC-CM) might be able to bridge the gap, provided the cells reproduce typical characteristics of human atrial myocardium. Retinoic acid (RA) has been introduced into cardiac differentiation protocols for the induction of an atrial phenotype in hiPSC-CM.[17,18] The exposure of hiPSC to RA during cardiac differentiation changed the expression from a ventricular to a more atrial pattern. The effectiveness of RA to induce an atrial phenotype could be confirmed by several different groups.[19–24] However, both the parameters used to quantify atrialisation and the degree of similarity to adult human atrium differed widely. Previous atrial-like hiPSC-CM (hiPSC-aCM) missed the large impact of atrial-selective potassium currents on repolarisation.[17,25–27] The present study presents a technical improvement of hiPSC atrial differentiation which results in action potentials (AP) closely replicating human atrial electrophysiology. In these hiPSC-aCM, PITX2 deficiency was associated with some characteristics known from persistent AF in patients and animal models.

Methods

The data that support the findings of this study are available from the corresponding author upon reasonable request. This investigation conforms to the principles outlined by the Declaration of Helsinki. Skin fibroblasts were taken with informed consent of the donors. All procedures involving the generation and analysis of hiPSC lines were approved by the local ethics committee in Hamburg (Az PV4798, 28.10.2014). A detailed description of the methods (including statistics) is provided in the Supplementary material online. In brief, a complete knock-out between exons 3 and 7 of the *PITX2* gene was performed in a healthy hiPS control cell line (isogenic control) to establish a new *PITX2*-deficient hiPSC line (PITX2$^{-/-}$). Both hiPSC lines were differentiated with an improved atrial differentiation protocol and hiPSC-aCM of PITX2$^{-/-}$ and isogenic control were cultured in atrial engineered heart tissue (aEHT). Expression analysis was performed by RNA-sequencing. Force and action potentials were measured in intact aEHT.[28] Ion currents were recorded in isolated hiPSC-aCM at 37 °C.[29]

Results

Effective knock out of *PITX2* in aEHT

Effective knock out of *PITX2* was confirmed by mRNA sequencing (**Figure 1**) and Western blot (**Supplement Figure 4**). As depicted in the regional plot of the genomic region surrounding PITX2 (**Figure 1**), mRNA expression of the regular PITX2 transcript was completely lost in the hiPSC lines after deletion. Of note, an enhanced transcription of parts of exon 1 was observed in these hiPSC lines, likely due to the complex regulatory framework of this genomic region.[6]

PITX2 deficiency reduces contraction force

Spontaneous beating of aEHT was monitored by video-optical measurements over time of aEHT culture. PITX2$^{-/-}$ aEHT started to beat later during development (16±1 vs. 12±1 days, n=28/3 vs. n=28/4, PITX2$^{-/-}$ vs. isogenic control; p=0.002, unpaired t-test, **Figure 2A**). After 30 days of culture beating rate was slightly lower in PITX2$^{-/-}$ than controls (135.2±21.3 vs. 147.1±11 bpm, n=28/3 vs. n=28/4, PITX2$^{-/-}$ vs. isogenic control; p=0.01, nested t-test). RR scatter, as a measure of beating irregularity, was not different at any point of the entire period of aEHT culture (**Figure 2D**). However, in PITX2$^{-/-}$ force at day 30 amounted only to about 40% of controls (0.053±0.015 vs. 0.131±0.017 mN, n=28/3 vs. n=28/4, PITX2$^{-/-}$ vs. isogenic control; p<0.0001, nested t-test) and the time to 80% relaxation (RT_{80}) in PITX2$^{-/-}$ was longer (0.22±0.06 vs. 0.13±0.04 s, n=28/3 vs. n=28/4, PITX2$^{-/-}$ vs. isogenic control; p=0,004, nested t-test, **Supplement Figure 6**).

PITX2 deficiency induces lower I_{Kur} and action potential triangulation

AP in isogenic control aEHT showed the typical AP shape of human atrium (**Figure 3C**) consisting of a strong initial repolarisation followed by a plateau at quite negative voltage. Interestingly, PITX2$^{-/-}$ aEHT showed a more triangular AP shape. Specifically, APD_{20} was much longer (40±12.6 vs. 7.5±4.4 ms, n=26/4 vs. n=21/6, PITX2$^{-/-}$ vs. isogenic control; p<0.0001, nested t-test; **Figure 3C**) and no clear plateau was present. APD_{90} was slightly, but significantly shorter in PITX2$^{-/-}$ aEHT (140.6±14.5 vs. 163.1±31 ms, n=26/4 vs. n=21/6, PITX2$^{-/-}$ vs. isogenic control; p=0.008 nested t-test; **Figure 3G**). The plateau voltage ($V_{Plateau}$; **Figure 3H**) was significantly higher in the PITX2$^{-/-}$ vs. isogenic controls (3.2±6.6 vs. -18.7±5.5 mV, n=26/4 vs. n=21/6, PITX2$^{-/-}$ vs. isogenic control; p<0.0001, nested t-test). Maximum diastolic potential (MDP) was more negative in PITX2$^{-/-}$ (-77.55±4.6 vs. -70.8±2.8 mV, n=26/4 vs. n=21/6, PITX2$^{-/-}$ vs. control; p<0.0001, nested t-test; **Figure 3D**). The latter finding was associated with higher action potential amplitude (APA; 102.7±6 vs. 91.1±10.9 mV, n=26/4 vs.

n=21/6, PITX2$^{-/-}$ vs. isogenic control; p<0.0001, nested t-test) and a faster maximum upstroke velocity (dV/dt_{max}) in PITX2$^{-/-}$ (232.3±76.6 vs. 161±76 V/s, n=26/4 vs. n=21/6, PITX2$^{-/-}$ vs. isogenic control; p=0.03, nested t-test; **Figure 3E**). Burst stimulation was applied in n=8 aEHTs from PITX2$^{-/-}$ and n=8 aEHTs from isogenic controls. We could not induce any arrhythmias neither in controls nor in PITX2$^{-/-}$.

Smaller effects of I_{Kur} block in PITX2$^{-/-}$

Early repolarisation of human atrial myocardium is dominated by large, rapidly activating transient outward currents that are smaller in AF-remodelled atria than in sinus rhythm (SR).[30] A low concentration of the potassium channel blocker 4-aminopyridine (4-AP, 50 μM) was used to estimate the contribution of I_{Kur} to repolarisation. In isogenic controls, 4-AP increased APD_{20} (from 7.5± 4.4 to 32.8±10.4 ms, n=17/6; p<0.0001, paired t-test), but shortened APD_{90} (from 163.4±34.1 to 128.9±5.7 ms, n=17/6, p=0.0004, paired t-test; **Figure 4A-D**). This seemingly paradoxal effect of 4-AP on APD_{90} is typical for atrial myocardium and explained by shift of the plateau and concomitant activation of I_{Kr}.[31] Indeed, 4-AP shifted the $V_{Plateau}$ to more positive values (from -18.1±6.3 to 3.1±11.2 mV, n=17/6; p<0.0001, paired t-test; **Figure 4F**). MDP was more negative in the presence of 4-AP and consequently APA and dV/dt_{max} were larger (**Supplement Table 5.2**). All of these effects of low concentrations of 4-AP have been observed in human atria previously.[31] In PITX2$^{-/-}$, 4-AP effects clearly differed. 4-AP increased APD_{20} by the same absolute amount, but starting from much larger basal values (from 48.4±8.1 to 68.2±6.1 ms, n=22/4; p<0.0001, paired t-test, relative increase to 141±56% of predrug values vs. 437±161% in isogenic controls, p<0.0001, nested t-test; **Figure 4C**). In contrast to isogenic controls, APD_{90} was prolonged by 4-AP in PITX2$^{-/-}$ (from 151.8±24.6 to 167.5±17.3 ms, n=22/4; p<0.0001, paired t-test; **Figure 4D**). 4-AP increased the $V_{Plateau}$ in PITX2$^{-/-}$ aEHT (from 4.1±2.1 to 11.1±2.1 mV, n=22/4; p<0.0001, paired t-test), but the effect was much smaller than in isogenic controls (**Figure 4E**). In stark contrast to isogenic controls, MDP, APA and dV/dt_{max} were not changed by 4-AP in PITX2$^{-/-}$ (**Supplement Table 5.2**). In order to substantiate our assumption that smaller effects of 4-AP on AP shape in PITX2$^{-/-}$ relates to smaller transient outward currents we performed patch clamp experiments. Outward currents at +50 mV showed the typical combination of large peak and sustained outward currents. Peak currents were clearly smaller in

PITX2$^{-/-}$ (Figure X). In addition, block of peak currents by 50 µM 4-AP was clearly smaller in PITX2$^{-/-}$ than in isogenic controls (5.5±5.0 vs. 21.6±23.4 pA/pF, $p<0.05$ n=57/2 vs. 36/2).

Activation of muscarinic receptors shortens APD in both PITX2$^{-/-}$ and controls but hyperpolarization is lost in PITX2$^{-/-}$

Activation of muscarinic receptors shortens APD and hyperpolarizes the MDP in human atrium, but both effects are almost lost in AF-remodelled human atria.[32] In isogenic controls, carbachol (CCh) shortened APD_{90} (from 157.1±12.1 to 83.4±2 ms, n=14/6; $p<0.0001$, paired t-test; **Figure 5A-C**), hyperpolarized MDP (from -70.1±0.9 to -82.5±2.3 mV, n=14/6; $p<0.0001$, paired t-test; **Figure 5D**) and slowed beating rate as expected (from 147.5±16.1 to 83.7±14.1, n=14/6; $p<0.0001$, paired t-test; **Figure 5E**). CCh also shortened APD_{90} in PITX2$^{-/-}$ (from 146.5±12.7 to 103.7±14.3 ms, n=14/3; $p<0.0001$, paired t-test) and slowed the beating rate (from 143.4±5.6 to 81.7±4.5 bpm, n=16/4; $p<0.0001$, paired t-test), but did not affect MDP (**Figure 5C-E**). A possible explanation for the blunted effect of $I_{K,ACh}$ activation on MDP could be that the MDP in PITX2$^{-/-}$ is already so much closer to the Nernst potential of potassium than in control that the contribution of additional potassium conductance becomes irrelevant. Indeed, *in silico* data obtained with an established computational human atrial CM model suggest that to be a plausible explanation (**Supplement Figure 7**). That is, a further activation of $I_{K,ACh}$ on top of I_{K1} augmentation induces only a negligible change in MDP (-0.2 mV) compared to the control case (-4.3 mV).

Ca^{2+} current density is smaller in PITX2$^{-/-}$

In AF-remodelled human atria, the reduction in force is associated with a reduction in I_{Ca}.[33] Therefore, PITX2$^{-/-}$ hiPSC-CM were subjected to measurements of I_{Ca} by patch clamping. Cell capacitance was smaller in PITX2$^{-/-}$ (25.7±8.1 vs. 37.4±17 pF, n=139/3 vs. n=143/3, PITX2$^{-/-}$ vs. isogenic control; $p<0.0001$, nested t-test). $I_{Ca,L}$ density was smaller in PITX2$^{-/-}$ (2.2±1.4 vs. 3.6±2.3 pA/pF, n=37/3 vs. n=33/3, PITX2$^{-/-}$ vs. isogenic control; $p<0.0001$, nested t-test, **Figure 6B**), whereas $I_{Ca,T}$ densities did not differ.

More negative MDP in PITX2$^{-/-}$ is not associated with higher I_{K1}

Given the role of I_{K1} in stabilizing MDP, the more negative MDP in PITX2$^{-/-}$ could be associated with higher I_{K1} densities. Unexpectedly, I_{K1} was not significantly different between PITX2$^{-/-}$ and isogenic controls (**Supplement Figure 8**). Furthermore, CCh effects were preserved in PITX2$^{-/-}$ (see above). Since measuring of ion currents in hiPSC-CM can be technically challenging[34], a computational modelling approach was performed to estimate how much stronger I_{K1} would have to be to produce the experimentally observed negative shift in MDP in PITX2$^{-/-}$. For this purpose, a mathematical model of the human atrial CM was used.[35] The simulation results indicate that I_{K1} would need to be about four times stronger than in control to produce a –8.6 mV shift in the MDP (**Supplement Figure 7**), unlikely to be overlooked.

Expression analysis with RNA-sequencing

To characterize the transcriptional landscape of PITX2$^{-/-}$ vs. isogenic control hiPSC lines, RNA sequencing was performed and 2,234 differentially expressed transcripts were discovered at a 2-fold log change and an adjusted P-value<0.05 after correction for multiple testing (842 transcripts upregulated, 1,349 transcripts downregulated (**Figure 7A**). Among these, extracellular matrix organization (adj. P=1.03e^{-60}) and muscle contraction (adj. P=1.21e^{-13}) were observed. 29 genes were selected coding for ion channels and transporters influencing the atrial AP (**Figure 7B**). In parallel to reduced $I_{Ca,L}$ density and force generation, transcripts encoding proteins regulating calcium homeostasis like ATP2A2 (SERCA2), ATP2B2 (plasma membrane Ca-ATPase), CACNA1C ($I_{Ca,L}$), RYR2 (ryanodine receptor) and SLC8A1 (Na-Ca-Exchanger) were less abundant in PITX2$^{-/-}$. In contrast, expression of ATP1A3 (α_3-subunit of the sodium-potassium ATPase) was increased in PITX2$^{-/-}$. KCNJ4 (subunit of I_{K1}) was significantly more abundant, whereas the abundance of all other transcripts of subunits coding for I_{K1} (KCNJ12, KCNJ14, KCNJ2) did not differ between PITX2$^{-/-}$ vs. isogenic control (**Figure 7B**).

Discussion

Rapid electrical activation of the atria during AF induces electrical remodelling that is characterized by shortening of APD and decrease in I_{Ca}.[36] This study demonstrates that complete ablation of PITX2,

a gene associated with increased incidence of AF, associates with some aspects of electrical remodelling as seen in AF, but in the absence of rapid electrical activity.

Improved atrial EHT as a model for human atrium

There is a considerable interest in hiPSC-CM as a model for atrial electrophysiology.[37] Retinoic acid (RA) induces an atrial phenotype in hiPSC-CM.[17,21,26,38] Previous studies showed atrial-specific expression of ion channels as an indication for an atrial phenotype. Although RA-treated hiPSC-CM showed typical markers of atrial myocardium,[17,21,26,27,38] the electrophysiological characteristics of the human atrium were incompletely reproduced. In particular, previous atrial hiPSC-CM missed the very strong early repolarisation followed by a plateau clearly below 0 mV.[17,21,26,39] AP in RA-treated EHT but not control (ventricular) EHT responded to I_{Kur} block.[17,26] However, effects of I_{Kur} block were modest,[17,26] suggesting that I_{Kur} density of previous atrial-like hiPSC-CMs was substantially smaller than in freshly isolated human atrial myocytes as confirmed by recent patch clamp studies.[25] Furthermore, there were also some discrepancies regarding the late repolarisation in former atrial hiPSC-CM. APD shortening upon activation of muscarinic receptors was very small compared to human atrial tissue.[17,26]

In this study, aEHT showed improved atrial-like AP characteristics, including a strong early repolarisation phase followed by a very low plateau voltage (-19.2 mV), very similar to human atrial tissue (-21mV)[31]. Furthermore, I_{Kur} block shifted the plateau voltage to positive values in aEHT and shortened APD_{90}, very similar to what has been described in human atrium.[31] Another improvement is the strong response of aEHT to muscarinic effects. The inward rectifier currents were doubled upon CCh, associated with marked hyperpolarization and substantial APD shortening. Given that the present data were obtained by the same group of investigators in the same laboratory with the same hiPSC line,[26,27] subtle methodological issues must have been responsible for the better present results. Both studies employed 1 µM RA for atrial differentiation, but sterile filtered it in the previous and not so in the current study. Indeed, mass spectrometric determination of RA concentrations before and after sterile filtration showed that more than 90% of RA was bound to filters (data not shown). The data indicate that the true concentration of RA in our previous studies was at least 10-fold lower than intended and that the use of 1 µM RA was key to the better atrial phenotype. We have investigated

concentration-dependent effects of RA on atrial differentiation. In addition, we have systematically studied loss of RA by sterile filtration. Results are published in preliminary form.[40]

I_{Ca} and force are decreased in PITX2$^{-/-}$

A decrease in $I_{Ca,L}$ is one of the key findings of AF[41,42] and is associated with smaller force.[43,44] $I_{Ca,L}$ was also reduced in homozygous PITX2 knock out atrial myocytes.[11] The reduced $I_{Ca,L}$ in the mouse model is likely associated with lower force, but corresponding data are missing. In this study, the reduction in $I_{Ca,L}$ current and transcript abundance in the mouse model[11] could be confirmed in human aEHTs. The reduction in $I_{Ca,L}$ in PITX2$^{-/-}$ hiPSC-aCM (by 40%) is similar to reduction found in CM isolated from patients with AF (by 50%,).[41,42] Smaller $I_{Ca,L}$ and force in PITX2$^{-/-}$ hiPSC-aCM/aEHT suggest the possibility that $I_{Ca,L}$ is under direct or indirect control of PITX2. It seems reasonable that the reduction in $I_{Ca,L}$ in AF patients with low PITX2 can be, at least in part, a direct consequence of low PITX2 levels and not necessarily only the consequence of AF remodelling. This would suggest that atrial force can be reduced in patients with low PITX2 levels before AF arises. Obviously, more work is needed to substantiate this hypothesis. This seems to be warranted, because primarily reduced contractility of the atria may have clinical implications. It could facilitate thrombus formation and be one reason why PITX2 gene variants are associated with embolic stroke.[45]

Effect of PITX2$^{-/-}$ on AP remodelling

In heterozygous PITX2 deficient mice, APD was shorter but only at pacing rates >600/min.[10,46] The relevance for human cardiac electrophysiology is difficult to judge, since such high rates cannot be reached in a human setting. Shortening of atrial APD is a key finding in patients with AF.[47] However, due to a blunted rate adaptation (shortening) of APD in AF, the difference in APD_{90} between SR and AF declines at faster rates and is no longer present above 3 Hz.[47] In our study with hiPSC-aCM, APD_{90} was only slightly shorter in PITX2$^{-/-}$. However, it remains unclear whether APD_{90} would have been significantly shorter in PITX2$^{-/-}$ aEHTs at low rate due to the spontaneous beating of aEHT above 2 Hz.

In murine atria, repolarisation is rather monotonic resulting in a more triangular AP shape.[16] In human atrium, a rapid initial phase of repolarisation is followed by a plateau phase resulting in a 10-times

longer APD_{90}.[31] Importantly, electrical remodelling in patients with AF does not only affect total repolarisation (expressed as APD_{90}), but also early repolarisation (APD_{20}). The contribution of transient potassium outward currents is smaller in patients with AF,[30,48] resulting in a prolongation of APD_{20}, which was observed not only at 1 Hz but also at pacing rates as high as 5 Hz.[49] The current findings show that PITX2 deficiency in hiPSC-aCM produces remodelling of early repolarisation which resembles AP remodelling in persistent AF.

We were not able to induce arrhythmias by burst stimulation in our aEHT model. In contrast, arrhythmias can be easily induced by burst pacing in ring-shaped aEHT, even in controls.[21,50] The data suggest that ring-shaped EHT may be a better model to study reentry tachycardia.

Weaker early repolarisation: a common link in genetic AF?

Rare mutations[51] and common gene variants[52] in *KCNA5* are associated with AF in humans, suggesting that defects in early repolarisation may contribute to the development of AF. Mutations in *KCNA5* found in patients with early AF resulted in smaller I_{Kur} currents measured in heterologous expression systems.[52,53] In the present study, KCNA5 transcript abundance was not altered in PITX2$^{-/-}$ compared to isogenic controls. Nevertheless, the drastic prolongation of APD_{20} in PITX2$^{-/-}$ aEHTs and the smaller 4-AP effect strongly imply that I_{Kur} must be reduced in PITX2$^{-/-}$ aEHT. Like in human AF, slowing of early repolarization in PITX2$^{-/-}$ was associated with a marked reduction of transient outward currents.

More negative diastolic potential in PITX2$^{-/-}$

In AF-remodelled human atria, mean RMP was found to be 3 mV more negative than in SR.[54] The more negative RMP in persistent AF was associated with two times higher I_{K1} density,[32] which suggests a causal relationship. Of note, MDP in PITX2$^{-/-}$ aEHT was almost 9 mV more negative than in isogenic controls. The validity of this finding is supported by the observation that the more negative MDP in PITX2$^{-/-}$ was associated with larger dV/dt_{max} and APA. If I_{K1} would be exclusively responsible for the more negative MDP, the current density had to be roughly 4-fold higher, as suggested by the computer simulations. However, I_{K1} density was not different in PITX2. Another finding also argues for different contribution of potassium currents to repolarisation. While $I_{K,ACh}$ was

well preserved, APD shortening upon CCh was smaller in PITX2$^{-/-}$, hyperpolarization was lost. Several other ion currents can contribute to MDP, e.g. sodium-potassium ATPase which we found higher expressed on mRNA level (ATP1A3 encoding for α3-subunit). In isogenic controls, block of sodium-potassium ATPase with 200 nM ouabain hyperpolarized MDP (data not shown). Thus, we expect other, rather complex reasons for the more negative MDP in PITX2$^{-/-}$.

Limitations

This study explored the consequences of total deficiency of PITX2, a scenario which does not or only rarely occur in patients. Instead, PITX2 transcripts appear to be reduced in LA samples from patients with persistent AF[13]. However, PITX2 transcript levels in left atrial cardiomyocytes showed a large scatter.[55] Thus, the mechanistic relation between the gene variants close to the *PITX2* gene and AF still remain unclear.[8] It cannot be excluded that alterations other than or in addition to decreased PITX2 abundance account for the electrophysiological phenotype, e.g. altered interplay between the neighbouring genes and PITX2 such as PANCR or ENPEP.[6,56] In any case, direct consequences of the relative PITX2 deficiency are likely smaller than reported in our study. The consequences of PITX2 deletion were investigated in hiPSC-CM with their inherent limitations in maturity.[57] However, the AP characteristics of hiPSC-derived aEHTs were surprisingly adult-like, arguing for good validity. In addition, the model allows the dissection of cause-effect relations independent of any confounding factors such as age, stretch, fibrosis and high rate. One shortcoming of the immature phenotype of aEHTs is the high basal beating rate which may have obscured effects on APD_{90}. Another is the contamination of calcium currents by $I_{Ca,T}$, which has been already observed earlier in ventricular EHT, whereas the contribution to total calcium influx is expected to be rather minor.

Perspective

Electrical remodelling in human persistent AF is believed to result from rapid electrical activation of the atria. Complete PITX2 deficiency in hiPSC-aCM recapitulates some typical findings of electrical remodelling in the absence of fast beating, indicating that at least some of these abnormalities could be primary consequences of low PITX2 levels. Atrial EHTs are able to reproduce key characteristics of human atrial electrophysiology and can be used for gene editing with CRISPR/Cas9. AP recordings in aEHT expressing clinically relevant variants next to *PITX2* should be compared to *in vivo* monophasic

AP recordings in the very same affected patients. Provided aEHT may reproduce findings in patients, hiPSC-aCM could serve as a model to study contribution of ion channels to PITX2-related phenotypes. In order to clarify whether clinically relevant reduced PITX2 levels in cardiomyocytes[55] may have an impact on atrial electrophysiology studying concentration-dependency of PITX2 effects on aEHT should be helpful.

Acknowledgements

The authors gratefully acknowledge expert technical assistance of Anna Steenpaß. Authors thank all members of the hiPSC-CM working group at the Department of Experimental Pharmacology and Toxicology, UKE-Hamburg, for their support with stem cell culture and hiPSC-CM differentiation.

Conflict of interest

T.E. is consultant and shareholder of Dinaqor AG.

Data availability

The RNA sequencing data were deposited to the GEO repository (accession no.: GSE175944). All other data underlying this article will be shared on reasonable request to the corresponding author.

Funding

The work was supported by a grant provided by the German Centre for Cardiovascular Research (grant no. 81Z0710110 to C.S.), by the European Research Council (ERC-AG IndivuHeart) by DZHK Postdoc Start-up Grant (grant no. 81X3710108 to M. D. L.) and by the Research Promotion Fund of the Faculty of Medicine (Hamburg, “Clinician Scientist Program” to M. D. L.).

Supplemental Material

Supplemental Methods

Supplemental Tables I-V

Supplemental Figures I-VIII

References [57-75]

References

1. Kornej, J., Börschel, C. S., Börschel, C. S., Benjamin, E. J., Benjamin, E. J., Schnabel, R. B. & Schnabel, R. B. Epidemiology of Atrial Fibrillation in the 21st Century: Novel Methods and New Insights. *Circ. Res.* **127**, 4–20 (2020).

2. Schotten, U., Verheule, S., Kirchhof, P. & Goette, A. Pathophysiological mechanisms of atrial fibrillation: A translational appraisal. *Physiological Reviews* vol. 91 265–325 at https://doi.org/10.1152/physrev.00031.2009 (2011).

3. Selzer, A. & Cohn, K. E. Natural history of mitral stenosis: a review. *Circulation* **45**, 878–890 (1972).

4. Kannel, W. B., Wolf, P. A., Benjamin, E. J. & Levy, D. Prevalence, Incidence, Prognosis, and Predisposing Conditions for Atrial Fibrillation: Population-Based Estimates. *Am. J. Cardiol.* **82**, 2N-9N (1998).

5. Roselli, C., Rienstra, M. & Ellinor, P. T. Genetics of Atrial Fibrillation in 2020: GWAS, Genome Sequencing, Polygenic Risk, and Beyond. *Circulation research* vol. 127 21–33 at https://doi.org/10.1161/CIRCRESAHA.120.316575 (2020).

6. Aguirre, L. A., Alonso, M. E., Badía-Careaga, C., Rollán, I., Arias, C., Fernández-Miñán, A., López-Jiménez, E., Aránega, A., Gómez-Skarmeta, J. L., Franco, D., *et al.* Long-range regulatory interactions at the 4q25 atrial fibrillation risk locus involve PITX2c and ENPEP. *BMC Biol.* **13**, 1–13 (2015).

7. Gudbjartsson, D. F., Arnar, D. O., Helgadottir, A., Gretarsdottir, S., Holm, H., Sigurdsson, A., Jonasdottir, A., Baker, A., Thorleifsson, G., Kristjansson, K., *et al.* Variants conferring risk of atrial fibrillation on chromosome 4q25. *Nature* **448**, 353–357 (2007).

8. Van Ouwerkerk, A. F., Hall, A. W., Kadow, Z. A., Lazarevic, S., Reyat, J. S., Tucker, N. R., Nadadur, R. D., Bosada, F. M., Bianchi, V., Ellinor, P. T., *et al.* Epigenetic and Transcriptional Networks Underlying Atrial Fibrillation. *Circ. Res.* 34–50 (2020) doi:10.1161/CIRCRESAHA.120.316574.

9. Gore-Panter, S. R., Hsu, J., Hanna, P., Gillinov, A. M., Pettersson, G., Newton, D. W., Moravec, C. S., Van Wagoner, D. R., Chung, M. K., Barnard, J., *et al.* Atrial Fibrillation associated chromosome 4q25 variants are not associated with PITX2c expression in human adult left atrial appendages. *PLoS One* **9**, e86245 (2014).

10. Syeda, F., Holmes, A. P., Yu, T. Y., Tull, S., Kuhlmann, S. M., Pavlovic, D., Betney, D., Riley, G., Kucera, J. P., Jousset, F., *et al.* PITX2 Modulates Atrial Membrane Potential and the Antiarrhythmic Effects of Sodium-Channel Blockers. *J. Am. Coll. Cardiol.* **68**, 1881–1894 (2016).

11. Lozano-Velasco, E., Hernández-Torres, F., Daimi, H., Serra, S. A., Herraiz, A., Hove-Madsen, L., Aránega, A. & Franco, D. Pitx2 impairs calcium handling in a dose-dependent manner by modulating Wnt signalling. *Cardiovasc. Res.* **109**, 55–66 (2016).

12. Kirchhof, P., Kahr, P. C., Kaese, S., Piccini, I., Vokshi, I., Scheld, H. H., Rotering, H., Fortmueller, L., Laakmann, S., Verheule, S., *et al.* PITX2c is expressed in the adult left atrium, and reducing Pitx2c expression promotes atrial fibrillation inducibility and complex changes in gene expression. *Circ. Cardiovasc. Genet.* **4**, 123–133 (2011).

13. Chinchilla, A., Daimi, H., Lozano-Velasco, E., Dominguez, J. N., Caballero, R., Delpón, E., Tamargo, J., Cinca, J., Hove-Madsen, L., Aranega, A. E., *et al.* PITX2 insufficiency leads to atrial electrical and structural remodeling linked to arrhythmogenesis. *Circ. Cardiovasc.*

Genet. **4**, 269–279 (2011).

14. Wang, J., Bai, Y., Li, N., Ye, W., Zhang, M., Greene, S. B., Tao, Y., Chen, Y., Wehrens, X. H. T. & Martin, J. F. Pitx2-microRNA pathway that delimits sinoatrial node development and inhibits predisposition to atrial fibrillation. *Proc. Natl. Acad. Sci. U. S. A.* **111**, 9181–9186 (2014).

15. Lin, C. R., Kloussi, C., O'Connell, S., Briata, P., Szeto, D., Liu, F., Izpisúa-Belmonte, J. C. & Rosenfeld, M. G. Pitx2 regulates lung asymmetry, cardiac positioning and pituitary and tooth morphogenesis. *Nature* **401**, 279–282 (1999).

16. Nerbonne, J. M. Mouse models of arrhythmogenic cardiovascular disease: Challenges and opportunities. *Curr. Opin. Pharmacol.* **15**, 107–114 (2014).

17. Devalla, H. D., Schwach, V., Ford, J. W., Milnes, J. T., El-Haou, S., Jackson, C., Gkatzis, K., Elliott, D. A., Chuva de Sousa Lopes, S. M., Mummery, C. L., *et al.* Atrial-like cardiomyocytes from human pluripotent stem cells are a robust preclinical model for assessing atrial-selective pharmacology. *EMBO Mol. Med.* **7**, 394–410 (2015).

18. Prabhu, S., Voskoboinik, A., McLellan, A. J. A., Peck, K. Y., Pathik, B., Nalliah, C. J., Wong, G. R., Azzopardi, S. M., Lee, G., Mariani, J., *et al.* Biatrial Electrical and Structural Atrial Changes in Heart Failure: Electroanatomic Mapping in Persistent Atrial Fibrillation in Humans. *JACC Clin. Electrophysiol.* **4**, 87–96 (2018).

19. Argenziano, M., Lambers, E., Hong, L., Sridhar, A., Zhang, M., Chalazan, B., Menon, A., Savio-Galimberti, E., Wu, J. C., Rehman, J., *et al.* Electrophysiologic Characterization of Calcium Handling in Human Induced Pluripotent Stem Cell-Derived Atrial Cardiomyocytes. *Stem Cell Reports* **10**, 1867–1878 (2018).

20. Shaheen, N., Shiti, A., Huber, I., Shinnawi, R., Arbel, G., Gepstein, A., Setter, N., Goldfracht, I., Gruber, A., Chorna, S. V., *et al.* Human Induced Pluripotent Stem Cell-Derived Cardiac Cell Sheets Expressing Genetically Encoded Voltage Indicator for Pharmacological and Arrhythmia Studies. *Stem Cell Reports* **10**, 1879–1894 (2018).

21. Goldfracht, I., Protze, S., Shiti, A., Setter, N., Gruber, A., Shaheen, N., Nartiss, Y., Keller, G. & Gepstein, L. Generating ring-shaped engineered heart tissues from ventricular and atrial human pluripotent stem cell-derived cardiomyocytes. *Nat. Commun.* **11**, 1–15 (2020).

22. Gunawan, M. G., Sangha, S. S., Shafaattalab, S., Lin, E., Heims-Waldron, D. A., Bezzerides, V. J., Laksman, Z. & Tibbits, G. F. Drug screening platform using human induced pluripotent stem cell-derived atrial cardiomyocytes and optical mapping. *Stem Cells Transl. Med.* **10**, 68–82 (2021).

23. Honda, Y., Li, J., Hino, A., Tsujimoto, S. & Lee, J. K. High-Throughput Drug Screening System Based on Human Induced Pluripotent Stem Cell-Derived Atrial Myocytes ~ A Novel Platform to Detect Cardiac Toxicity for Atrial Arrhythmias. *Front. Pharmacol.* **12**, 1–12 (2021).

24. Pei, F., Jiang, J., Bai, S., Cao, H., Tian, L., Zhao, Y., Yang, C., Dong, H. & Ma, Y. Chemical-defined and albumin-free generation of human atrial and ventricular myocytes from human pluripotent stem cells. *Stem Cell Res.* **19**, 94–103 (2017).

25. Hilderink, S., Devalla, H. D., Bosch, L., Wilders, R. & Verkerk, A. O. Ultrarapid Delayed Rectifier K+ Channelopathies in Human Induced Pluripotent Stem Cell-Derived Cardiomyocytes. *Front. Cell Dev. Biol.* **8**, 1–14 (2020).

26. Lemme, M., Ulmer, B. M., Lemoine, M. D., Zech, A. T. L., Flenner, F., Ravens, U., Reichenspurner, H., Rol-Garcia, M., Smith, G., Hansen, A., *et al.* Atrial-like Engineered Heart Tissue: An In Vitro Model of the Human Atrium. *Stem Cell Reports* **11**, 1378–1390 (2018).

27. Lemoine, M. D., Lemme, M., Ulmer, B. M., Braren, I., Krasemann, S., Hansen, A., Kirchhof, P., Meyer, C., Eschenhagen, T. & Christ, T. Intermittent optogenetic tachypacing of atrial engineered heart tissue induces only limited electrical remodelling. *J. Cardiovasc. Pharmacol.* **77**, 291–299 (2021).

28. Lemoine, M. D., Krause, T., Koivumäki, J. T., Prondzynski, M., Schulze, M. L., Girdauskas, E., Willems, S., Hansen, A., Eschenhagen, T. & Christ, T. Human Induced Pluripotent Stem Cell-Derived Engineered Heart Tissue as a Sensitive Test System for QT Prolongation and Arrhythmic Triggers. *Circ. Arrhythmia Electrophysiol.* **11**, 1–15 (2018).

29. Lemme, M., Braren, I., Prondzynski, M., Aksehirlioglu, B., Ulmer, B. M., Schulze, M. L., Ismaili, D., Meyer, C., Hansen, A., Christ, T., *et al.* Chronic intermittent tachypacing by an optogenetic approach induces arrhythmia vulnerability in human engineered heart tissue. *Cardiovasc. Res.* (2019) doi:10.1093/cvr/cvz245.

30. Van Wagoner, D. R., Pond, A. L., McCarthy, P. M., Trimmer, J. S. & Nerbonne, J. M. Outward K+ current densities and Kv1.5 expression are reduced in chronic human atrial fibrillation. *Circ. Res.* **80**, 772–781 (1997).

31. Wettwer, E., Hála, O., Christ, T., Heubach, J. F., Dobrev, D., Knaut, M., Varró, A. & Ravens, U. Role of IKur in controlling action potential shape and contractility in the human atrium: Influence of chronic atrial fibrillation. *Circulation* **110**, 2299–2306 (2004).

32. Dobrev, D., Graf, E., Wettwer, E., Himmel, H. M., Hála, O., Doerfel, C., Christ, T., Schüler, S. & Ravens, U. Molecular basis of downregulation of G-protein -coupled inward rectifying k+ current (ik,ach) in chronic human atrial fibrillation decrease in GIRK4 mrna correlates with reduced IK,ACh and muscarinic receptor-mediated shortening of action potentials. *Circulation* **104**, 2551–2557 (2001).

33. Christ, T., Rozmaritsa, N., Engel, A., Berk, E., Knaut, M., Metzner, K., Canteras, M., Ravens, U. & Kaumann, A. Arrhythmias, elicited by catecholamines and serotonin, vanish in human chronic atrial fibrillation. *Proc Natl Acad Sci U S A* **111**, 11193–11198 (2014).

34. Horváth, A., Lemoine, M. D., Löser, A., Mannhardt, I., Flenner, F., Uzun, A. U., Neuber, C., Breckwoldt, K., Hansen, A., Girdauskas, E., *et al.* Low Resting Membrane Potential and Low Inward Rectifier Potassium Currents Are Not Inherent Features of hiPSC-Derived Cardiomyocytes. *Stem Cell Reports* **10**, 822–833 (2018).

35. Koivumäki, J. T., Seemann, G., Maleckar, M. M. & Tavi, P. In Silico Screening of the Key Cellular Remodeling Targets in Chronic Atrial Fibrillation. *PLoS Comput. Biol.* **10**, 1003620 (2014).

36. Allessie, M., Ausma, J. & Schotten, U. Electrical, contractile and structural remodeling during atrial fibrillation. *Cardiovasc. Res.* **54**, 230–246 (2002).

37. Christ, T., Lemoine, M. D. & Eschenhagen, T. Are atrial human pluripotent stem cell-derived cardiomyocytes ready to identify drugs that beat atrial fibrillation? *Nat. Commun.* **12**, 10–12 (2021).

38. Cyganek, L., Tiburcy, M., Sekeres, K., Gerstenberg, K., Bohnenberger, H., Lenz, C., Henze, S., Stauske, M., Salinas, G., Zimmermann, W. H., *et al.* Deep phenotyping of human induced pluripotent stem cell-derived atrial and ventricular cardiomyocytes. *JCI insight* **3**, (2018).

39. Borchert, T., Hübscher, D., Guessoum, C. I., Lam, T. D. D., Ghadri, J. R., Schellinger, I. N., Tiburcy, M., Liaw, N. Y., Li, Y., Haas, J., *et al.* Catecholamine-Dependent β-Adrenergic Signaling in a Pluripotent Stem Cell Model of Takotsubo Cardiomyopathy. *J. Am. Coll. Cardiol.* **70**, 975–991 (2017).

40. https://doi.org/10.1101/2023.01.03.522611 (2023).

41. Van Wagoner, D. R., Pond, A. L., Lamorgese, M., Rossie, S. S., McCarthy, P. M. & Nerbonne, J. M. Atrial L-type Ca2+ currents and human atrial fibrillation. *Circ. Res.* **85**, 428–436 (1999).

42. Christ, T., Boknik, P., Wöhrl, S., Wettwer, E., Graf, E. M. M., Bosch, R. F. F., Knaut, M., Schmitz, W., Ravens, U. & Dobrev, D. L-type Ca2+ current downregulation in chronic human atrial fibrillation is associated with increased activity of protein phosphatases. *Circulation* **110**, 2651–2657 (2004).

43. Schotten, U., Ausma, J., Stellbrink, C., Sabatschus, I., Vogel, M., Frechen, D., Schoendube, F., Hanrath, P. & Allessie, M. A. Cellular mechanisms of depressed atrial contractility in patients with chronic atrial fibrillation. *Circulation* **103**, 691–698 (2001).

44. Christ, T., Rozmaritsa, N., Engel, A., Berk, E., Knaut, M., Metzner, K., Canteras, M., Ravens, U. & Kaumann, A. Arrhythmias, elicited by catecholamines and serotonin, vanish in human chronic atrial fibrillation. *Proc. Natl. Acad. Sci. U. S. A.* **111**, 11193–11198 (2014).

45. Bevan, S., Traylor, M., Adib-Samii, P., Malik, R., Paul, N. L. M., Jackson, C., Farrall, M., Rothwell, P. M., Sudlow, C., Dichgans, M., *et al.* Genetic heritability of ischemic stroke and the contribution of previously reported candidate gene and genomewide associations. *Stroke* **43**, 3161–3167 (2012).

46. Nadadur, R. D., Broman, M. T., Boukens, B., Mazurek, S. R., Yang, X., van den Boogaard, M., Bekeny, J., Gadek, M., Ward, T., Zhang, M., *et al.* Pitx2 modulates a Tbx5-dependent gene regulatory network to maintain atrial rhythm. *Sci. Transl. Med.* **8**, 354ra115 (2016).

47. Franz, M. R., Karasik, P. L., Li, C., Moubarak, J. & Chavez, M. Electrical remodeling of the human atrium: Similar effects in patients with chronic atrial fibrillation and atrial flutter. *J. Am. Coll. Cardiol.* **30**, 1785–1792 (1997).

48. Christ, T., Wettwer, E., Voigt, N., Hála, O., Radicke, S., Matschke, K., Várro, A., Dobrev, D. & Ravens, U. Pathology-specific effects of the IKur/Ito/IK,ACh blocker AVE0118 on ion channels in human chronic atrial fibrillation. *Br. J. Pharmacol.* **154**, 1619–1630 (2008).

49. Ford, J., Milnes, J., El Haou, S., Wettwer, E., Loose, S., Matschke, K., Tyl, B., Round, P. & Ravens, U. The positive frequency-dependent electrophysiological effects of the IKur inhibitor XEN-D0103 are desirable for the treatment of atrial fibrillation. *Hear. Rhythm* **13**, 555–564 (2016).

50. Laksman, Z., Wauchop, M., Lin, E., Protze, S., Lee, J., Yang, W., Izaddoustdar, F., Shafaattalab, S., Gepstein, L., Tibbits, G. F., *et al.* Modeling Atrial Fibrillation using Human Embryonic Stem Cell-Derived Atrial Tissue. *Sci. Rep.* **7**, 1–11 (2017).

51. Tao, G., Kahr, P. C., Morikawa, Y., Zhang, M., Rahmani, M., Heallen, T. R., Li, L., Sun, Z., Olson, E. N., Amendt, B. A., *et al.* Pitx2 promotes heart repair by activating the antioxidant response after cardiac injury. *Nature* **534**, 119–123 (2016).

52. Christophersen, I. E., Olesen, M. S., Liang, B., Andersen, M. N., Larsen, A. P., Nielsen, J. B., Haunsø, S., Olesen, S.-P., Tveit, A., Svendsen, J. H., *et al.* Genetic variation in KCNA5: impact on the atrial-specific potassium current IKur in patients with lone atrial fibrillation.

Eur. Heart J. **34**, 1517–1525 (2013).

53. Olson, T. M., Alekseev, A. E., Liu, X. K., Park, S., Zingman, L. V, Bienengraeber, M., Sattiraju, S., Ballew, J. D., Jahangir, A. & Terzic, A. Kv1.5 channelopathy due to KCNA5 loss-of-function mutation causes human atrial fibrillation. *Hum. Mol. Genet.* **15**, 2185–2191 (2006).

54. Ravens, U., Katircioglu-Öztürk, D., Wettwer, E., Christ, T., Dobrev, D., Voigt, N., Poulet, C., Loose, S., Simon, J., Stein, A., *et al.* Application of the RIMARC algorithm to a large data set of action potentials and clinical parameters for risk prediction of atrial fibrillation. *Med. Biol. Eng. Comput.* **53**, 263–273 (2015).

55. Reyat, J. S., Chua, W., Cardoso, V. R., Witten, A., Kastner, P. M., Nashitha Kabir, S., Sinner, M. F., Wesselink, R., Holmes, A. P., Pavlovic, D., *et al.* Reduced left atrial cardiomyocyte PITX2 and elevated circulating BMP10 predict atrial fibrillation after ablation. *JCI Insight* **5**, 1–16 (2020).

56. Qin, Y., Gao, P., Yu, S., Li, J., Huang, Y., Jia, D., Tang, Z., Li, P., Liu, F. & Liu, M. A large deletion spanning pitx2 and pancr in a chinese family with axenfeld-rieger syndrome. *Mol. Vis.* **26**, 670–678 (2020).

57. Weinberger, F., Mannhardt, I. & Eschenhagen, T. Engineering Cardiac Muscle Tissue: A Maturating Field of Research. *Circ. Res.* **120**, 1487–1500 (2017).

58. Breckwoldt K, Letuffe-Brenière D, Mannhardt I, Schulze T, Ulmer B, Werner T, Benzin A, Klampe B, Reinsch MC, Laufer S et al. Differentiation of cardiomyocytes and generation of human engineered heart tissue. *Nat Protoc* 2017;**12**:1177–1197.

59. Concordet JP, Haeussler M. CRISPOR: Intuitive guide selection for CRISPR/Cas9 genome editing experiments and screens. *Nucleic Acids Res* Oxford University Press; 2018;**46**:W242–W245.

60. Hansen A, Eder A, Bonstrup M, Flato M, Mewe M, Schaaf S, Aksehirlioglu B, Schworer A, Uebeler J, Eschenhagen T. Development of a Drug Screening Platform Based on Engineered Heart Tissue. *Circ Res* 2010;

61. Feyen DAM, McKeithan WL, Bruyneel AAN, Spiering S, Hörmann L, Ulmer B, Zhang H, Briganti F, Schweizer M, Hegyi B et al. Metabolic Maturation Media Improve Physiological Function of Human iPSC-Derived Cardiomyocytes. *Cell Rep* 2020;**32**.

62. Mannhardt I, Breckwoldt K, Letuffe-Brenière D, Schaaf S, Schulz H, Neuber C, Benzin A, Werner T, Eder A, Schulze T et al. Human Engineered Heart Tissue: Analysis of Contractile Force. *Stem Cell Reports* 2016;**7**:29–42.

63. Wettwer E, Christ T, Endig S, Rozmaritsa N, Matschke K, Lynch JJ, Pourrier M, Gibson JK, Fedida D, Knaut M, et al. The new antiarrhythmic drug vernakalant: Ex vivo study of human atrial tissue from sinus rhythm and chronic atrial fibrillation. *Cardiovasc Res* England; 2013;**98**:145–154.

64. Ford J, Milnes J, Wettwer E, Christ T, Rogers M, Sutton K, Madge D, Virag L, Jost N, Horvath Z, Matschke K, Varro A, Ravens U. Human electrophysiological and pharmacological properties of XEN-D0101: A novel atrial-selective Kv1.5/IKur inhibitor. *J Cardiovasc Pharmacol* 2013;**61**:408–415.

65. Ismaili D, Geelhoed B, Christ T. Ca2+ currents in cardiomyocytes: How to improve interpretation of patch clamp data? *Prog Biophys Mol Biol* Elsevier Ltd; 2020;**157**:33–39.

66. Koivumäki JT, Korhonen T, Tavi P. Impact of sarcoplasmic reticulum calcium release on calcium dynamics and action potential morphology in human atrial myocytes: A computational study. *PLoS Comput Biol* 2011;**7**.

67. Skibsbye L, Jespersen T, Christ T, Maleckar MM, Brink J van den, Tavi P, Koivumäki JT. Refractoriness in human atria: Time and voltage dependence of sodium channel availability. *J Mol Cell Cardiol* 2016;**101**.

68. Eisner DA. Pseudoreplication in physiology: More means less. *J Gen Physiol* 2021;**153**:1–5.

69. Statistical Analysis & Graphics Software. https://ncss-wpengine.netdna-ssl.com/wp-content/uploads/2012/09/ PASSUG1.pdf

70. Andrews S. FastQC: a quality control tool for high throughput sequence data. 2010. https://www.bioinformatics.babraham.ac.uk/projects/fastqc/

71. Bolger AM, Lohse M, Usadel B. Trimmomatic: A flexible trimmer for Illumina sequence data. *Bioinformatics* 2014;**30**:2114–2120.

72. Pertea M, Pertea GM, Antonescu CM, Chang TC, Mendell JT, Salzberg SL. StringTie enables improved reconstruction of a transcriptome from RNA-seq reads. *Nat Biotechnol* 2015;**33**:290–295.

73. Watanabe K, Taskesen E, Bochoven A Van, Posthuma D. Functional mapping and annotation of genetic associations with FUMA. *Nat Commun* Springer US; 2017;**8**:1–10.

74. Robinson JT, Thorvaldsdóttir H, Winckler W, Guttman M, Lander ES, Getz G, Mesirov JP. Integrative genomics viewer. Nat. Biotechnol. NIH Public Access; 2011. p. 24–26.

75. Morgenstern J, Fleming T, Kliemank E, Brune M, Nawroth P, Fischer A. Quantification of All-Trans Retinoic Acid by Liquid Chromatography-Tandem Mass Spectrometry and Association with Lipid Profile in Patients with Type 2 Diabetes. *Metabolites* 2021;**11**.

Legends to the figures

Figure 1: Confirmation of PITX2 knock-out by RNA-sequencing

Regional plot of the genomic region surrounding PITX2 shows mRNA expression of the PITX2 transcript is completely lost in the PITX2$^{-/-}$ hiPSC line (legend in figure) after deletion, regular PITX2 expression is observed in the isogenic control hiPSC. Red bars indicate cutting sites of CRSIPR/Cas9 enzymes of sgRNA1 and sgRNA2.

Figure 2: Effects of PITX2$^{-/-}$ on force, beating rate and beating irregularity

Means±SD of force during 4 week culture (**A**) and individual data points at day 31 (**B**). N/N indicates number of aEHT/number of batches. * $p<0.05$, nested t-test. Mean±SD of beating rate (**C**) and beating irregularity expressed as R-R-scatter (**D**) during 4-week culture.

Figure 3: Effects of PITX2$^{-/-}$ on action potential parameters of aEHT

Consecutive original action potentials (AP) (**A**) and single APs (**C**) recorded in aEHT from isogenic control and PITX2$^{-/-}$. Frequency-dependent effect on action potential duration at 90% repolarisation (APD_{90}, **B**). Summary of results (individual data points and mean±SD) for maximum diastolic potential (MDP, **D**), maximum upstroke velocity (dV/dt_{max},**E**) action potential duration at 20% repolarisation (APD_{20}, **F**) and 90% repolarisation (APD_{90},**G**), and plateau voltage ($V_{Plateau}$, **H**). For definition of plateau voltage see supplement. N/N indicates number of aEHT/number of batches. * $p<0.05$, nested t-test.

Figure 4: Diminished effects of I_{Kur} block in PITX2$^{-/-}$ aEHT

Original AP recorded in aEHT from isogenic control (**A**) and PITX2$^{-/-}$ (**B**) before and after exposure to 4-aminopyridine (4-AP, 50 µM). Summary of results (individual data points and mean±SD) for the 4-AP effect on APD_{20} (**C**), APD_{90} (**D**) and $V_{Plateau}$ (**E**). Data are expressed as delta values. N/N indicates number of aEHT/number of batches.* $p<0.05$, nested t-test.

Figure 5: Preserved APD shortening upon muscarinic receptor stimulation in PITX2$^{-/-}$ aEHT

Original AP recorded in aEHT from isogenic control (**A**) and PITX2$^{-/-}$ (**B**) before and after exposure to the muscarinic receptor agonist carbachol (CCh, 10 µM). Summary of results (individual data points and mean±SD) for the CCh effect on APD_{90} (**C**), MDP (**D**) and beating rate (**E**) analysed after 2 minutes of exposure. Data are expressed as delta values. N/N indicates number of aEHT/number of batches. * $p<0.05$, nested t-test.

Figure 6: Smaller $I_{Ca,L}$ and transient potassium outward currents in PITX2$^{-/-}$

IV relationship (**A**) for $I_{Ca,\,L}$ in isogenic control and PITX2$^{-/-}$ (mean±SD). Individual data points and means±SD (**B**) for $I_{Ca,L}$ analysed at +10 mV. Original current traces (**C**) for potassium outward current recorded in hiPSC-aCM from PITX2$^{-/-}$ and isogenic control. Individual data points for peak outward currents at +50 mV and means±SD (**D**). N/N indicates number of hiPSC-aCM/number of batches, * indicates $p<0.05$ for nested t-test after log transformation of data.

Figure 7: Differentially expressed genes in PITX2$^{-/-}$

Heatmap of all significantly ($p<0.05$) differentially expressed transcripts by RNA sequencing (**A**) of EHT from isogenic control (n=2) vs. PITX2$^{-/-}$ (n=3), clustered by average linkage (spearman rank order). Relative gene expression (mean±SD) as fold change of PITX2$^{-/-}$ (n=3) over isogenic control (n=2) assessed by RNA sequencing of known ion channels regulating the atrial action potential (* adjusted p-value<0.05, **B**).

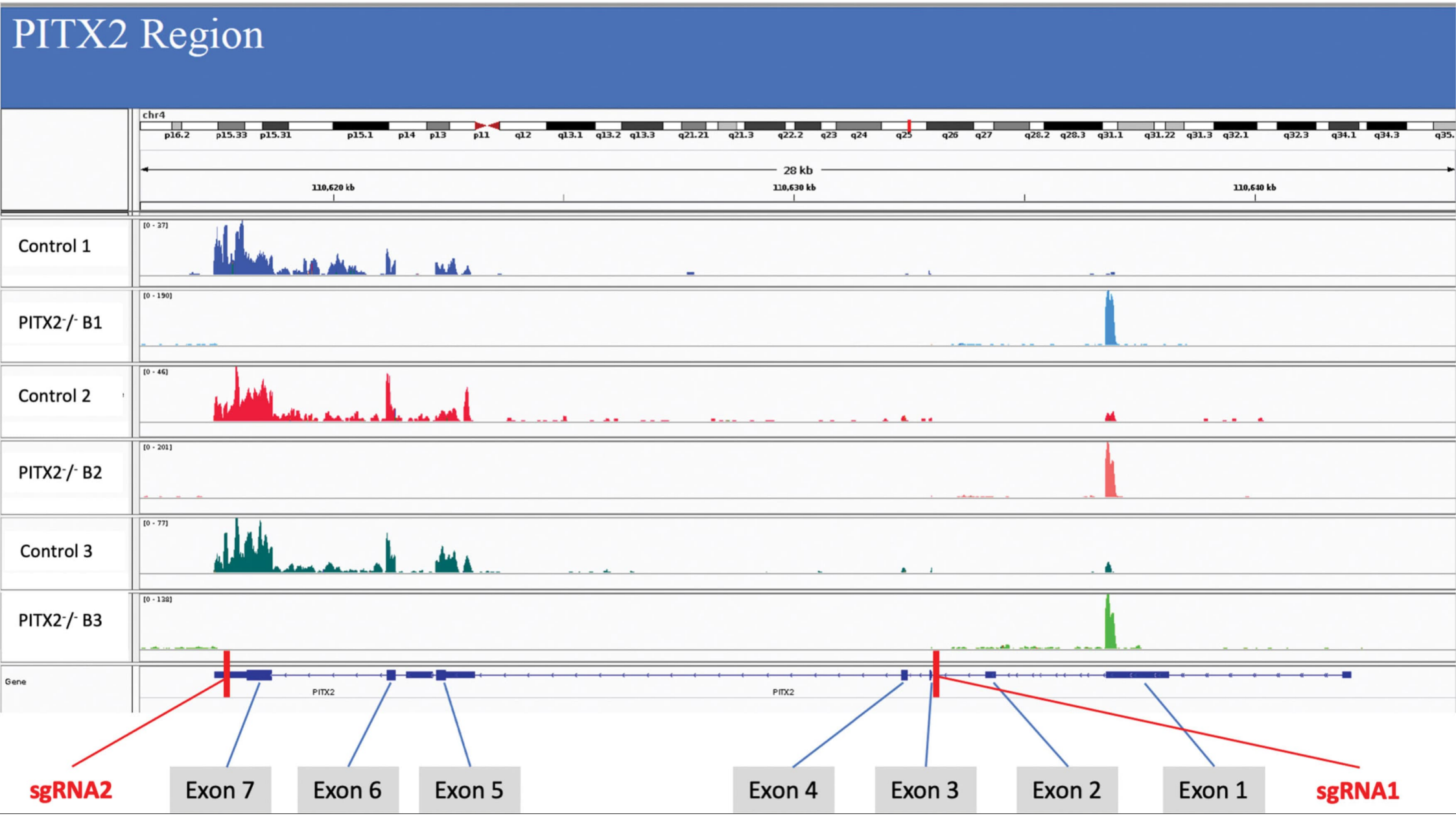
PITX2 Region
chr4
p16.2 p15.33 p15.31 p15.1 p14 p13 p11 q12 q13.1 q13.2 q13.3 q21.21 q21.3 q22.2 q23 q24 q25 q26 q27 q28.2 q28.3 q31.1 q31.22 q31.3 q32.1 q32.3 q34.1 q34.3 q35.
28 kb
110,620 kb
110,630 kb
110,640 kb
Control 1
[0 - 27]
PITX2-/- B1
[0 - 190]
Control 2
[0 - 46]
PITX2-/- B2
[0 - 201]
Control 3
[0 - 77]
PITX2-/- B3
[0 - 128]
Gene
PITX2
PITX2
sgRNA2
Exon 7
Exon 6
Exon 5
Exon 4
Exon 3
Exon 2
Exon 1
sgRNA1

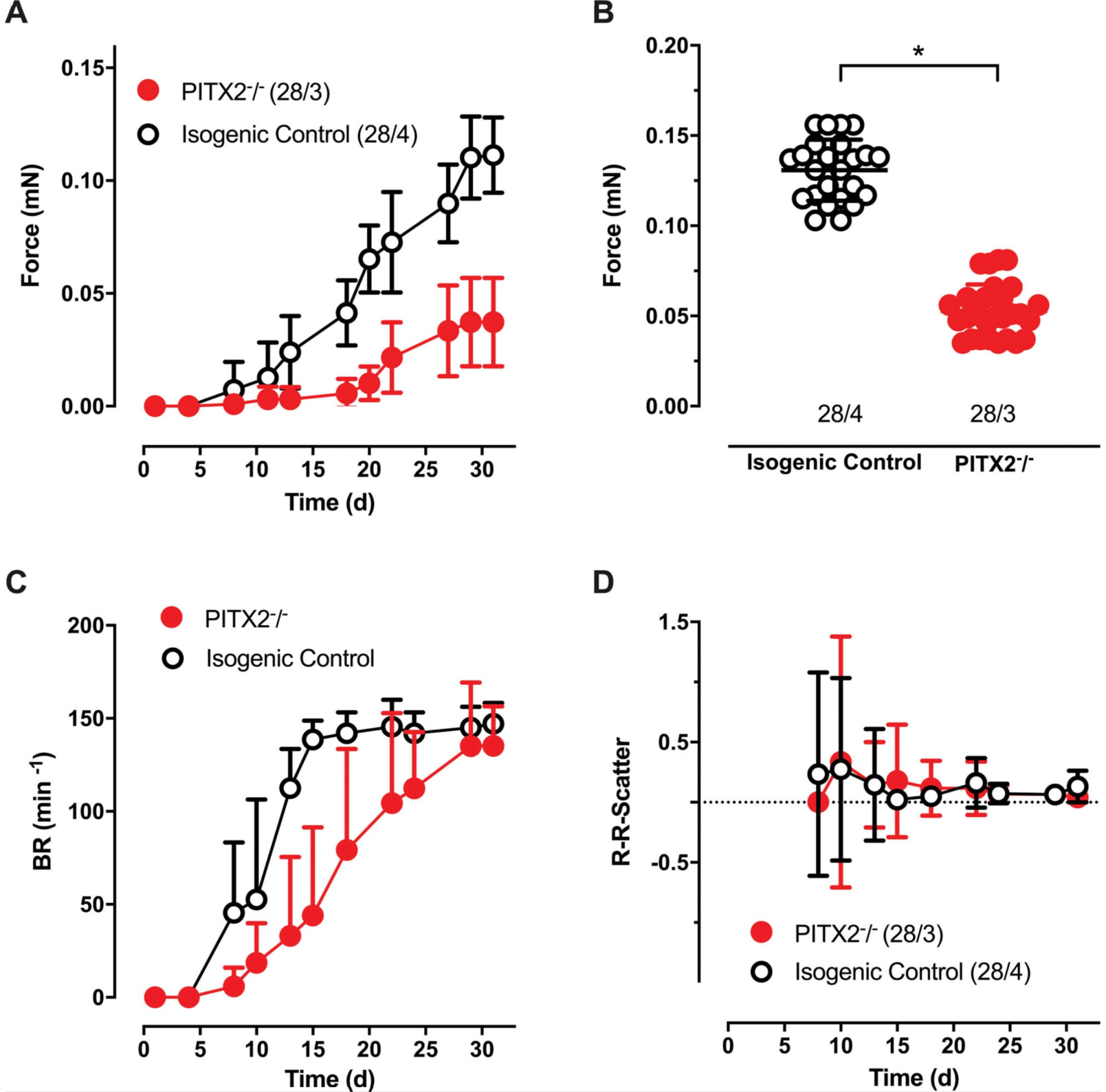
A
0.15
0.10
0.05
0.00
Force (mN)
PITX2-/- (28/3)
Isogenic Control (28/4)
0
5
10
15
20
25
30
Time (d)
B
0.20
0.15
0.10
0.05
0.00
Force (mN)
*
28/4
28/3
Isogenic Control
PITX2-/-
C
200
150
100
50
0
BR (min -1)
PITX2-/-
Isogenic Control
0
5
10
15
20
25
30
Time (d)
D
1.5
0.5
-0.5
R-R-Scatter
PITX2-/- (28/3)
Isogenic Control (28/4)
0
5
10
15
20
25
30
Time (d)

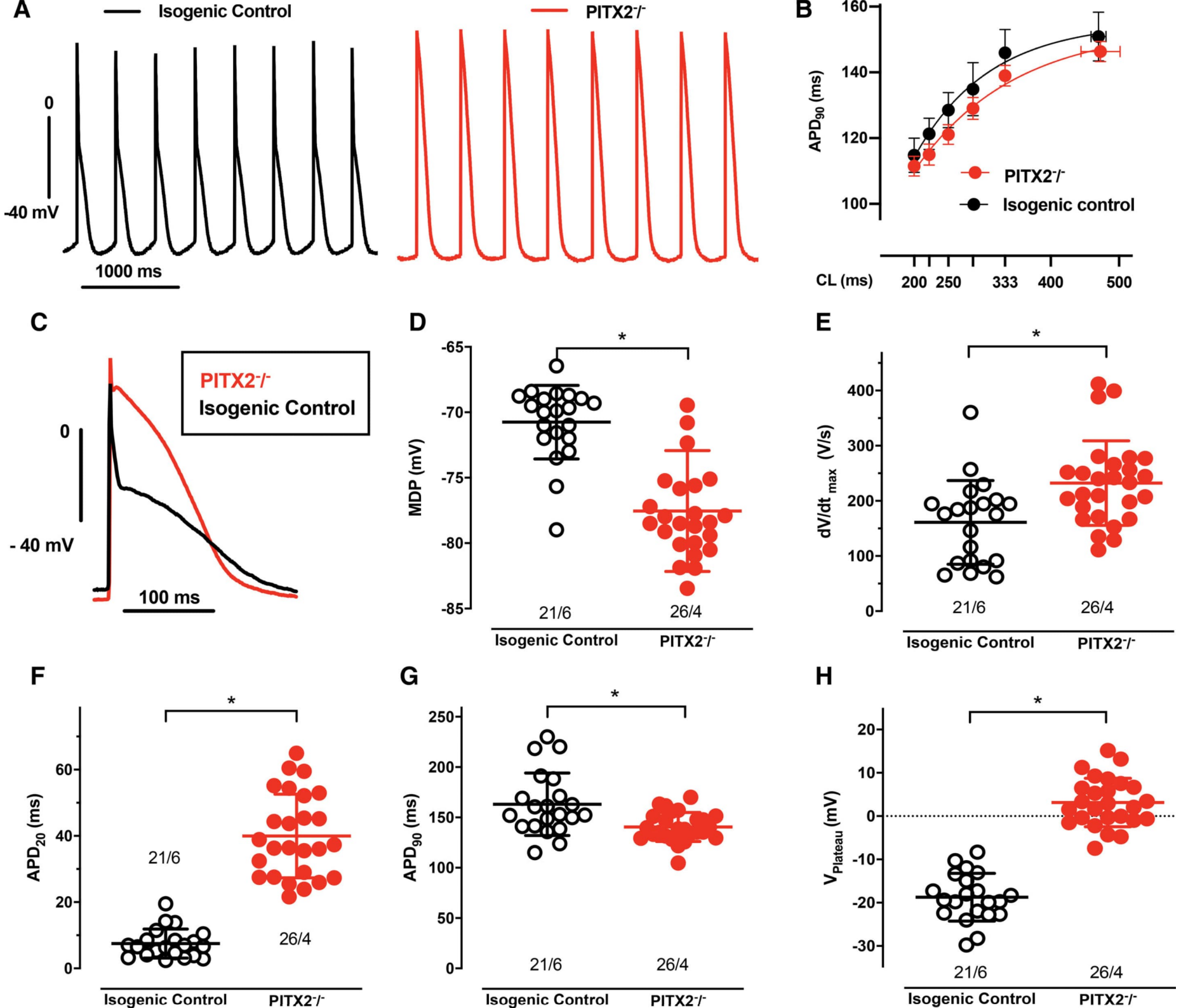
A
Isogenic Control
PITX2-/-
0
-40 mV
1000 ms
B
APD90 (ms)
160
140
120
100
PITX2-/-
Isogenic control
CL (ms)
200 250 333 400 500
C
PITX2-/-
Isogenic Control
0
- 40 mV
100 ms
D
MDP (mV)
-65
-70
-75
-80
-85
*
21/6
26/4
Isogenic Control
PITX2-/-
E
dV/dtmax (V/s)
400
300
200
100
0
*
21/6
26/4
Isogenic Control
PITX2-/-
F
APD20 (ms)
60
40
20
0
*
21/6
26/4
Isogenic Control
PITX2-/-
G
APD90 (ms)
250
200
150
100
50
0
*
21/6
26/4
Isogenic Control
PITX2-/-
H
VPlateau (mV)
20
10
0
-10
-20
-30
*
21/6
26/4
Isogenic Control
PITX2-/-

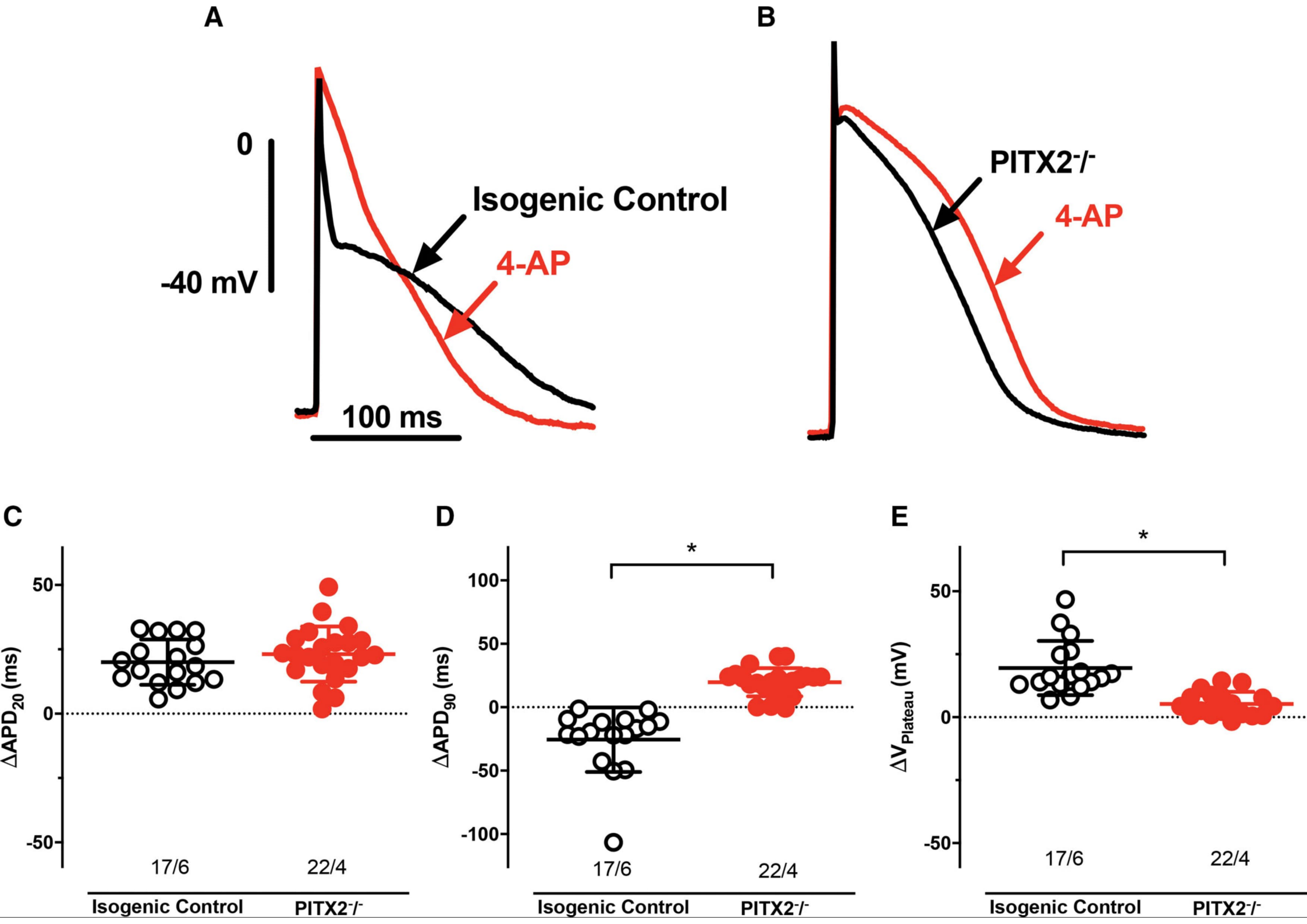
A
0
-40 mV
100 ms
Isogenic Control
4-AP
B
PITX2-/-
4-AP
C
ΔAPD20 (ms)
50
0
-50
17/6
22/4
Isogenic Control
PITX2-/-
D
ΔAPD90 (ms)
100
50
0
-50
-100
*
17/6
22/4
Isogenic Control
PITX2-/-
E
ΔVPlateau (mV)
50
0
-50
*
17/6
22/4
Isogenic Control
PITX2-/-

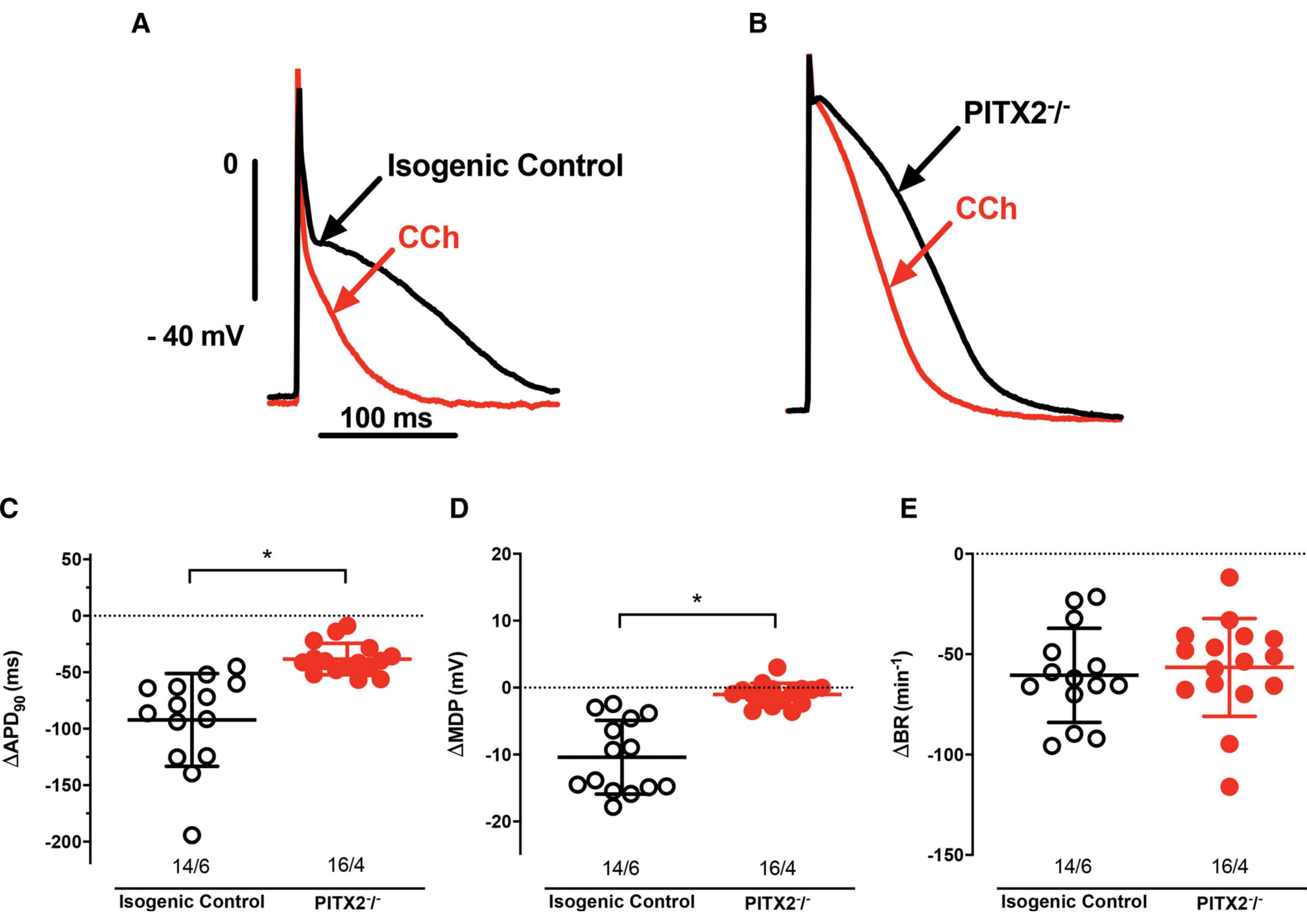
A
0
- 40 mV
Isogenic Control
CCh
100 ms
B
PITX2-/-
CCh
C
ΔAPD90 (ms)
50
0
-50
-100
-150
-200
*
14/6
16/4
Isogenic Control
PITX2-/-
D
ΔMDP (mV)
20
10
0
-10
-20
*
14/6
16/4
Isogenic Control
PITX2-/-
E
ΔBR (min-1)
0
-50
-100
-150
14/6
16/4
Isogenic Control
PITX2-/-

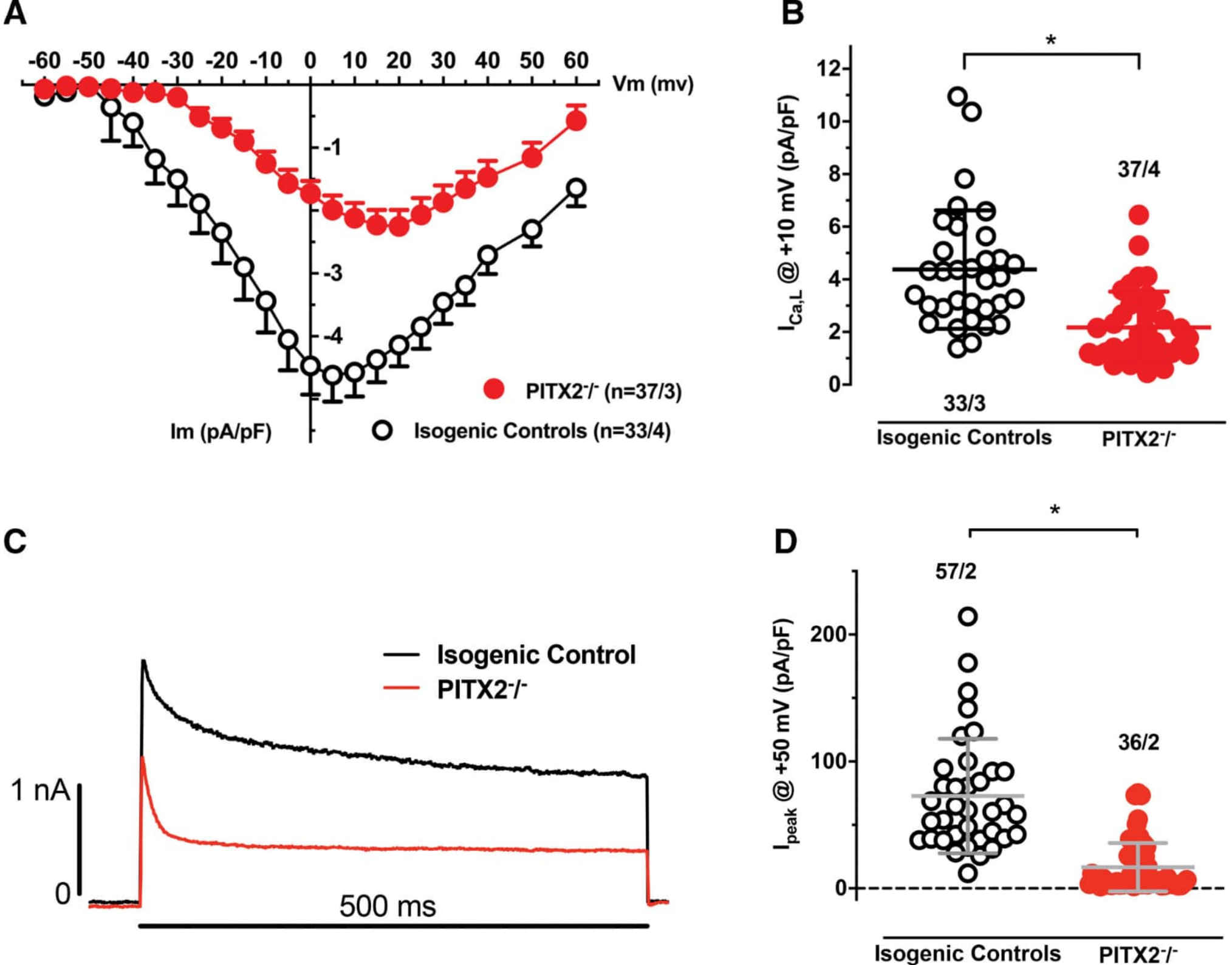
A
-60 -50 -40 -30 -20 -10 0 10 20 30 40 50 60
Vm (mv)
-1
-3
-4
PITX2-/- (n=37/3)
Im (pA/pF)
Isogenic Controls (n=33/4)
B
*
12
10
8
6
4
2
0
ICa,L @ +10 mV (pA/pF)
37/4
33/3
Isogenic Controls
PITX2-/-
C
Isogenic Control
PITX2-/-
1 nA
0
500 ms
D
*
57/2
200
100
0
Ipeak @ +50 mV (pA/pF)
36/2
Isogenic Controls
PITX2-/-

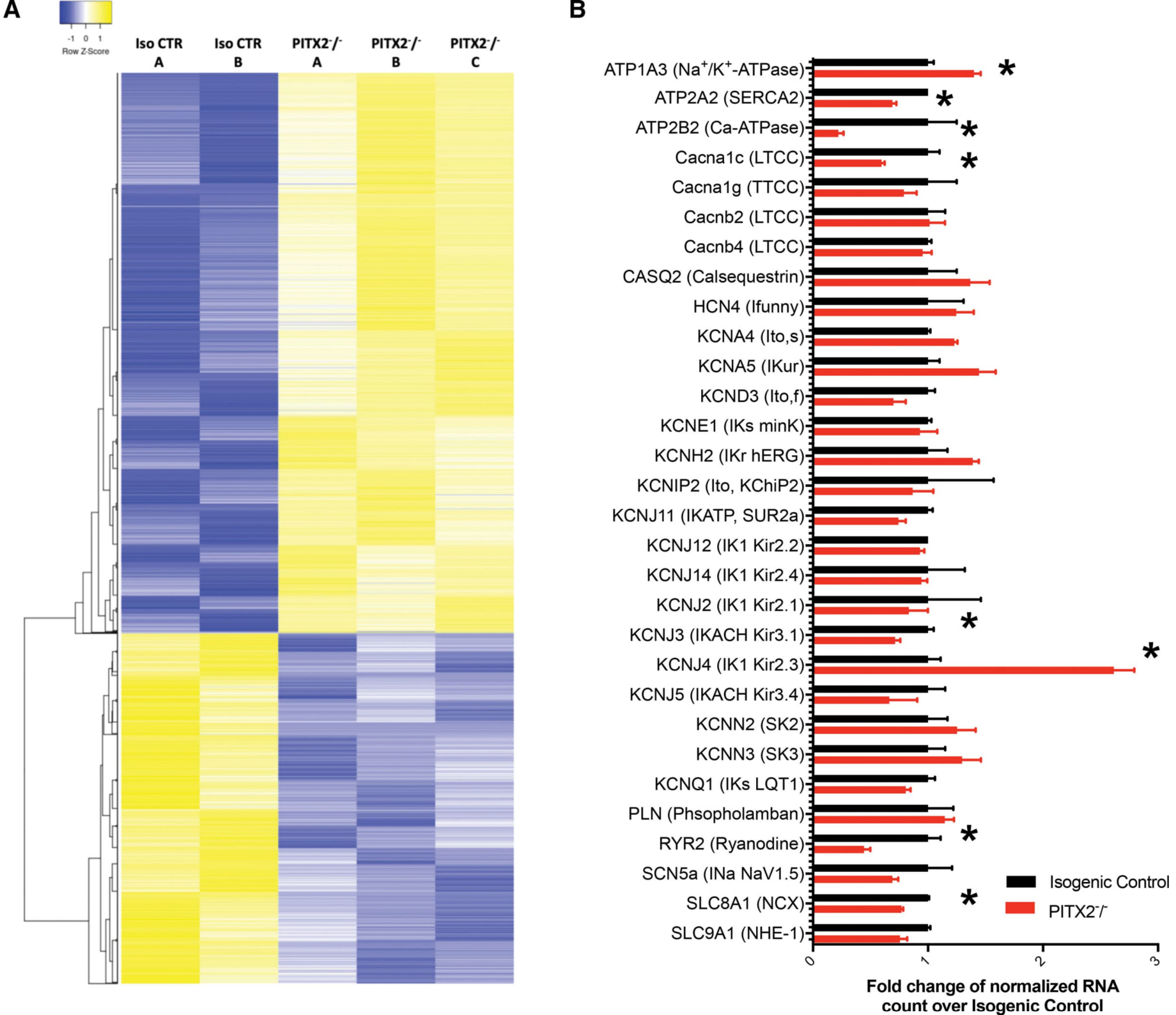
A
-1 0 1
Row Z-Score
Iso CTR A
Iso CTR B
PITX2-/- A
PITX2-/- B
PITX2-/- C
B
ATP1A3 (Na+/K+-ATPase)
ATP2A2 (SERCA2)
ATP2B2 (Ca-ATPase)
Cacna1c (LTCC)
Cacna1g (TTCC)
Cacnb2 (LTCC)
Cacnb4 (LTCC)
CASQ2 (Calsequestrin)
HCN4 (Ifunny)
KCNA4 (Ito,s)
KCNA5 (IKur)
KCND3 (Ito,f)
KCNE1 (IKs minK)
KCNH2 (IKr hERG)
KCNIP2 (Ito, KChiP2)
KCNJ11 (IKATP, SUR2a)
KCNJ12 (IK1 Kir2.2)
KCNJ14 (IK1 Kir2.4)
KCNJ2 (IK1 Kir2.1)
KCNJ3 (IKACH Kir3.1)
KCNJ4 (IK1 Kir2.3)
KCNJ5 (IKACH Kir3.4)
KCNN2 (SK2)
KCNN3 (SK3)
KCNQ1 (IKs LQT1)
PLN (Phsopholamban)
RYR2 (Ryanodine)
SCN5a (INa NaV1.5)
SLC8A1 (NCX)
SLC9A1 (NHE-1)
Isogenic Control
PITX2-/-
0
1
2
3
Fold change of normalized RNA count over Isogenic Control